


# Four-loop large- $n_f$ contributions to the non-singlet structure functions

**Conference Paper****Author(s):**

Pelloni, Andrea 

**Publication date:**

2024-01-22

**Permanent link:**

<https://doi.org/https://doi.org/10.3929/ethz-b-000659598>

**Rights / license:**

[Creative Commons Attribution-NonCommercial-NoDerivatives 4.0 International](#)

**Originally published in:**

PoS: Proceedings of Science 432, <https://doi.org/10.22323/1.432.0057>

## Four-loop large- $n_f$ contributions to the non-singlet structure functions

---

**A. Pelloni**<sup>a,\*</sup>

<sup>a</sup>ETH Zurich,

Ramistrasse 101, 8092 Zurich, Switzerland

E-mail: [apelloni@phys.ethz.com](mailto:apelloni@phys.ethz.com)

We present the progress in the computation of the unpolarized coefficient functions for Deep inelastic scattering. This computation completes the previous results for  $F_{2,L}$  for large- $n_f$  with the computation of the contributions to the charged current  $F_3$ . This additional structure function has contributions with color factor  $d^{abc}d_{abc}$ , and represents an increase in complexity for the construction of the differential equations used for the generation of the Mellin moments.

*16th International Symposium on Radiative Corrections: Applications of Quantum Field Theory to Phenomenology (RADCOR2023)*  
28th May - 2nd June, 2023  
Crieff, Scotland, UK

---

\*Speaker

## 1. Introduction

The determination of the structure functions for the inclusive deep-inelastic scattering (DIS) via the exchange of an electro-weak gauge boson is among the best studied processes in perturbative QCD both from the experimental and theoretical perspective. The structure functions have been determined with high accuracy over a wide range of energy scales  $Q^2$  of the exchanged boson in the electron-proton collider HERA ref. [1], and further experiments are being considered such as the Electron-Ion Collider (EIC) at Brookhaven National Lab [2, 3] and the Large Hadron Electron Collider (LHeC) [4, 5].

Precise determinations of the quark momentum distributions  $q_i(\xi, Q^2)$  (with  $\xi = x$  at the leading-order of perturbative QCD) as well as, less directly, of the gluon distribution  $g(\xi, Q^2)$  and the strong coupling  $\alpha_s$  from structure-function data, require higher-order calculations of the corresponding coefficient functions (partonic structure functions). These coefficient functions are of relevance also beyond the cross sections for inclusive DIS, see, e.g., refs. [6, 7] on Higgs production in vector-boson fusion and ref. [8] on jet production in DIS.

In this proceeding, we consider the flavour non-singlet contributions  $F_3$  structure function, the second-order corrections have been calculated and verified long ago [9–12]. The corresponding three-loop expressions were obtained in ref. [13] and recently re-calculated in ref. [14]. At the fourth order, only the lowest five Mellin- $N$  moments have been computed so far [15] using the FORCER program [16].

In the present article, we take the next step towards the determination of the fourth-order non-singlet coefficient functions  $c_{3,ns}^{(4)}(x)$  the leading and sub-leading contributions for the large- $n_f^2$  limit contributions. These results are obtained with the same method that was presented in ref. [17] for the computation of  $c_{L,ns}^{(4)}(x)$  and  $c_{2,ns}^{(4)}(x)$  for the extraction of a large number of moments, reaching (odd) values of  $N$  beyond  $N = 1000$ . Such a large number of moments is essential for sufficiently constraining the space of harmonic sums [18, 19] and re-construct the full analytic dependence in  $N$ , and hence on  $x$  in terms of harmonic polylogarithms (HPLs) [20].

The remainder of this article is organized as follows: In section 2 we briefly recall the theoretical framework for the coefficient functions in inclusive DIS and their determination of the fourth order in  $\alpha_s$ . In section 3 we review the method for the generation of the necessary Mellin moments [17]. The analytic results for the coefficient functions in  $N$ - and  $x$ -space are beyond the scope of this proceeding and are left for a soon-to-be-published paper. We summarize our method and results and give a brief outlook in section 4.

## 2. Theoretical framework and notations

The focus of this computation regards the computation of the spin-average hadronic tensor for the inclusive lepton-nucleon DIS,

$$\text{lepton}(k) + \text{nucleon}(p) \rightarrow \text{lepton}(k') + X \quad (1)$$

at lowest order in the weak current and fourth order in QCD, namely  $\mathcal{O}(\alpha \alpha_s^4)$ . The interaction happens through the exchange of a gauge boson with momentum  $q = k - k'$ , and the inclusive hadronic final state  $X$  consists of all contributions allowed by quantum number conservation. The

hadronic tensor factorized from the leptonic tensor in the cross section, and can be expressed as a function of the exchanged energy  $Q^2 = -q^2$  and the Bjorken variable  $x = \frac{Q^2}{2p \cdot q}$  in terms of the structure functions  $F_{L,2,3}$ ,

$$W_{\mu\nu}(p, q) = \frac{1}{4\pi} \int dz e^{iqz} \langle \text{nucl.}, p | J_\mu^\dagger(z) J_\nu(0) | \text{nucl.}, p \rangle \quad (2)$$

$$= e_{\mu\nu} \frac{1}{2x} F_L(x, Q^2) + d_{\mu\nu} \frac{1}{2x} F_2(x, Q^2) + i \epsilon_{\mu\nu\alpha\beta} \frac{p^\alpha q^\beta}{p \cdot q} F_3(x, Q^2) \quad (3)$$

with,

$$e^{\mu\nu} = g^{\mu\nu} + \frac{q^\mu q^\nu}{Q^2}, \quad d^{\mu\nu} = -g^{\mu\nu} + (p^\mu q^\nu + p^\nu q^\mu) \frac{2x}{Q^2} + p^\mu p^\nu \frac{4x^2}{Q^2}. \quad (4)$$

We presented the contribution to the first two structure functions for large  $n_f$  in ref. [17] and we now compute the expression for  $F_3$ , associated with the fully anti-symmetric tensor  $\epsilon_{\mu\nu\alpha\beta}$ . The coefficients can be extracted from the tensor by acting upon it with the appropriate Lorentz projector,

$$\mathbb{P}_3^{\mu\nu} = \frac{-i}{(d-2)(d-3)} \frac{2x}{Q^2} \epsilon^{\mu\nu\rho\sigma} p_\rho q_\sigma. \quad (5)$$

We use the optical theorem in a framework set out in refs. [21, 22] to associate the projection of the structure functions  $F_a$  of the hadronic tensor to the forward Compton scattering,

$$T_{\mu\nu}(p, q) = \frac{1}{4\pi} \int dz e^{iqz} \langle \text{nucl.}, p | T(J_\mu^\dagger(z) J_\nu(0)) | \text{nucl.}, p \rangle. \quad (6)$$

$$= e_{\mu\nu} \frac{1}{2x} \mathcal{T}_L(x, Q^2) + d_{\mu\nu} \mathcal{T}_2(x, Q^2) + i \epsilon_{\mu\nu\alpha\beta} \frac{p^\alpha q^\beta}{p \cdot q} \mathcal{T}_3(x, Q^2). \quad (7)$$

The relation between the Mellin moments of the structure functions and the scattering amplitude is given by,

$$\mathbf{M}[F_a](N) \approx \frac{1}{N!} \left[ \frac{d^N \mathcal{T}_a}{d1\omega^N} \right]_{\omega=0}, \quad (8)$$

for odd (even) values of  $N$  for  $F_3$  ( $F_{2,L}$ ) and the Mellin transform defined as,

$$\mathbf{M}[A(x)](N) = \int_0^1 dx x^{N-1} A(x). \quad (9)$$

The computation of  $F_3$  is associated with the vector/axial interference of the two weak currents. This interference also introduces a new complication due to the presence of  $\gamma_5$  and requiring extra care during renormalization. We employ the so-called Larin scheme to treat the presence of  $\gamma_5$ , rewriting the axial current as

$$\bar{\psi} \gamma_\mu \gamma_5 \psi \rightarrow i \frac{1}{6} \epsilon_{\mu\nu\rho\sigma} \bar{\psi} \gamma^\nu \gamma^\rho \gamma^\sigma \psi. \quad (10)$$

In order to recover the axial Ward-identity and taking into account the particular choice for the extension of  $\gamma_5$  into  $d$  dimensions, we require the use of the two renormalization constants  $Z_A$  and  $Z_5$  [23], which are known to up to four loops in the  $\overline{\text{MS}}$ -scheme [24].

We are interested in the partonic quantity  $C_{3,\text{ns}}$  related to the non-singlet combination of structure functions for  $F_{3,\text{ns}}$ , such as  $F_3^{\nu,\text{proton}} - F_3^{\nu,\text{neutron}}$ . The partonic quantity is related to the hadronic one by a simple Mellin convolution  $\otimes$  with the non-singlet combination of quark PDFs,

$$F_{3,\text{ns}}(x, Q^2) = [C_{3,\text{ns}} \otimes q_{\text{ns}}](x, Q^2). \quad (11)$$

The coefficient functions are expressed as an expansion in powers of the strong coupling constant  $a_s \equiv \alpha_s(Q^2)/(4\pi)$ ,

$$C_{3,\text{ns}}(x, Q^2) = \sum_{n=1} a_s^n c_{3,\text{ns}}^{(n)}(x). \quad (12)$$

Here and below we identify the  $\overline{\text{MS}}$  renormalization and mass-factorization scales  $\mu_r^2$  and  $\mu_f^2$ , at which the strong coupling and the PDFs are evaluated, with  $Q^2$ . The dependence on  $\mu_r^2$  and  $\mu_f^2$  can be readily reconstructed a posteriori, see, e.g., eqs. (2.17) and (2.18) of ref. [25]. The renormalized expression for the non-singlet case is simply given by,

$$C_{3,\text{ns}}^{\text{bare}} = C_{3,\text{ns}}(N, a_s) Z_{\text{ns}}(N, a_s). \quad (13)$$

The renormalization constant  $Z_{\text{ns}}$  of the non-singlet quark distribution depends only on the zeta function and the anomalous dimensions  $\gamma_{\text{ns}}$  that can be expressed in perturbative QCD as a series expansion in the strong coupling constant:

$$\gamma_{\text{ns}} = \sum_{l=0}^{\infty} a_s^{l+1} \gamma_{\text{ns}}^{(l)}, \quad a_s = \frac{\alpha_s}{4\pi} = \frac{g_s^2}{16\pi^2}. \quad (14)$$

The poles of the renormalization constant  $Z_{\text{ns}}$  are related to the anomalous dimensions, in particular the  $a_s^{l+1} \epsilon^{-1}$  contribution depends on the  $\gamma_{\text{ns}}^{(l)}$  anomalous dimension. This property can be exploited to extract the unknown splitting functions as the building blocks of the renormalization constant in the  $\overline{\text{MS}}$  scheme. The anomalous dimension at fixed  $N$  is related to the splitting function by a Mellin transform

$$\gamma_{\text{ns}}(N) = - \int_0^1 dx x^{N-1} P_{\text{ns}}. \quad (15)$$

In order to obtain the fourth-order coefficient functions  $c_{3,\text{ns}}^{(4)}$ , the lower-order calculations need to include terms up to  $\epsilon^{4-n}$  at order  $\alpha_s^n$  as well as a lower number of fermionic loops. In particular, the determination of the  $n_f^2$  contributions to  $c_{a,\text{ns}}^{(4)}$  requires the  $n_f$  parts of  $a_{a,\text{ns}}^{(3)}$ .

### 3. Method and computations

For the purpose of this computation we have followed the same methodology that we applied for the computation of  $F_L$  and  $F_2$  at fourth-order in perturbative QCD that was presented in ref. [17]. The treatment of the Feynman diagrams, up to the point where we apply the reduction to master integrals and set up the system of differential equations, is closely related to the third-order fermionic contributions in ref. [26] and the non-singlet part of ref. [27]. Our evaluation of the Feynman integrals is entirely different, though, from both. In ref. [27] the odd moments were computed to  $N=22$  for the  $C_F C_A n_f^2$  and  $d^{abc} d_{abc} / C_A n_f^2$  terms and to  $N=42$  for the  $C_F^2 n_f^2$  terms using FORCER [16]. By embedding the system with all available physics constraints and Diophantine

equations, it was only possible to access the analytic all- $N$  expression for the four-loop anomalous dimensions but not for the coefficient functions.

Below we discuss the details of the computation and give a review of the method employed for the first time in ref. [17]. Similarly to our previous results, we generate a large number of Mellin moments, up to  $N = 1500$ , to reconstruct the analytic  $N$ -dependence of the fourth-order coefficient functions by a direct (and over-constrained) Gaussian elimination for a sufficiently general ansatz in terms of harmonic sums.

Our setup relies on QGRAF [28] and FORM [29–31], utilizing the program MINOS [32] as a diagram database tool. Many of the FORM libraries we use have been employed in numerous previous calculations, as seen in references such as [12, 15, 26, 27, 33], and have been extensively optimized for multi-loop perturbative QCD computations. By organizing the diagrams in terms of similar topologies and color factors, it is possible to speed up the evaluation time by realizing algebraic cancellations at an early stage of the computation. The most complicated diagrams contributing to  $n_f^2$  do not include ‘genuine’ four-loop diagrams but always contain a fermionic self-energy correction to one of the gluon propagators, as illustrated in Fig. 1.

The generation of the Mellin moments of the partonic structure functions, related to the scattering amplitude via eq. (8), is performed via an expansion of the set of master integrals  $\vec{M}$ . In particular, the expansion coefficients are extracted using a system of differential equations around  $1/x \equiv \omega = 0$ , the inverse Bjorken variable.

### Series expansion and differential equations

The diagrams contributing to the final result are organized in terms of topologies of minimal complexity, where we favor the use of linear terms in the loop momenta as pure scalar products, compared to squared propagators. The relevant topologies are shown in Fig. 2, where only the squared propagator contribution are represented. The maximal complexity of the scalar integrals emerging from the diagrams is of 12 powers in the denominators together with a polynomial or order 4 in the loop momenta at the numerator. This represents a considerable increase in complexity for the reduction programs compared with the integrals appearing in the computation of  $F_{2,L}$ . To circumvent the prohibitive times required by general reduction to master integrals as implemented in dedicated public software, we employed a private code to combine integration-by-part (IBP) identities to express the few integrals that had the highest complexity (highest combined numerator and denominator powers) as a combination of simpler ones. This was primarily possible because of the limited number of high-complexity integrals, where we were able to quickly explore different

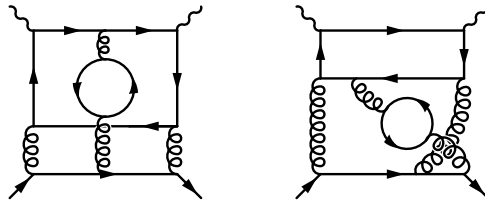


**Figure 1:** Some of the most complicated diagrams contributing to the computation for the  $n_f^2$  third-order coefficient functions for  $F_{3,ns}$ . All diagrams come with the color factor  $n_f^2 d^{abc} d_{abc} / n_c$ . When computing the boundary conditions, the first and second diagram will correspond to the BE and O4 topology in MINCER notation [34, 35] with a bubble insertion, respectively.

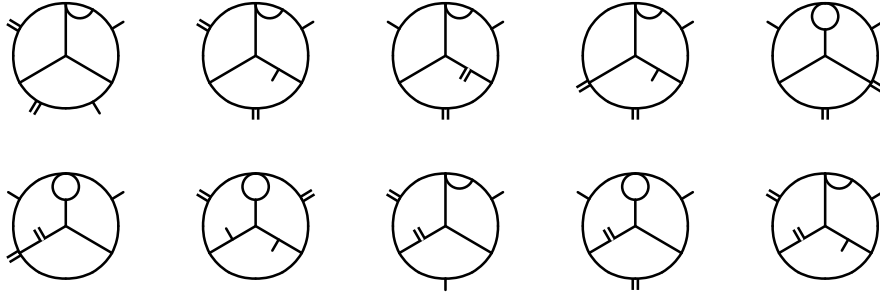


**Figure 2:** Four-loop propagator topologies used for the reduction to master integrals and the expansion in  $\omega$  using differential equations. The external double lines represent the off-shell exchanged bosons while the simple lines the parton related to the  $d^{abc}d_{abc}$  color factor. Each diagram allows for two independent flows of the external momenta resulting in the same topology up to a sign inversion  $\omega \leftrightarrow -\omega$ .

constraints on the selection of IBP identities to combine for performing the partial reduction of these integrals. Once obtained the simplified set of integrals, it is possible to delegate the last step of a full reduction to master integrals and the construction of a system of differential equations to FIRE. The resulting system of differential equations takes the form,

$$\frac{\partial}{\partial \omega} \vec{M}(\omega, \varepsilon) = A(\omega, \varepsilon) \cdot \vec{M}(\omega, \varepsilon), \quad (1)$$

where  $A \in \mathbb{Q}^{n \times n}(\omega, \varepsilon)$  is a square matrix whose elements are rational functions in  $\omega$  and the dimensional regulator  $\varepsilon$  over the field  $\mathbb{Q}$ , with  $n$  being the number of master integrals. We found that a simple rescaling of the masters by monomial coefficient in  $\omega$  is sufficient for making the regular singularity manifest in the differential system. We can then use a general ansatz for both the differential system and the master integrals to write down an iterative expression for the extraction of the unknown expansion coefficients of the master integrals,

$$\underbrace{((k+1)\mathbb{1} - A_{-1})}_{:= B_k} \cdot \vec{m}_{k+1} = \sum_{j=0}^k A_j \vec{m}_{k-j}, \quad (2)$$

$$M_i = \omega^{\alpha_i} \sum_{k=0}^{\infty} m_{ik} \omega^k, \quad A = \frac{A_{-1}}{\omega} + \sum_{k=0}^{\infty} A_k \omega^k, \quad (3)$$

where  $\mathbb{1}$  is the identity matrix. The singularities of the matrix  $B_k$  coincide with the positive integer eigenvalues of  $A_{-1}$ , nonetheless by keeping  $k$  a free parameter it is possible to write down a general expression for the inverse  $B_k^{-1}$ . For the finite number of  $k$ 's where it is not possible to invert the matrix  $B_k$ , we solve the system by means of Gaussian elimination, while for all other cases we rely on a recursive expression that only involves matrix multiplications,

$$\vec{m}_{k+1} = B_k^{-1} \cdot \left( \sum_{j_1+j_2=k} A_{j_1} \cdot \vec{m}_{j_2} \right). \quad (4)$$

The required boundary conditions have been computed using FORCER in the limit of  $\omega = 0$  for all the master integrals, where the external parton is taken to be soft. We used a C++ implementation

of Gaussian elimination to compute the first 10 orders of each master integral according to eq. (2) to clear past all  $k$ 's related to a singular  $B_k$ . For  $k > 10$  we used a FORM implementation of eq. (4). With this implementation we were able to obtain  $O(\omega^{1500})$  out of the differential equations within no more than a few days, making the reduction to master integrals by far the most demanding part of the computation, ranging to about a month for all 10 topologies. Such a large number of coefficients is required to sufficiently constrain the ansatz of harmonic sums and rational coefficients resulting in the reconstruction of the coefficient functions in  $N$ -space. The full expression for the coefficients will be presented in full in an upcoming publication together with the full  $x$ -space result for the  $n_f^2$  and  $n_f^3$  to the DIS coefficient functions.

#### 4. Conclusions

We present the framework used for the computation of the analytic for the odd- $N$  valued expression of the coefficient function  $F_3$  contributing to the  $n_f^2$  and  $n_f^3$  terms at four loops. We implement a new tailored reduction to tackle the increased complexity in the diagrams required reduction to master integrals. We observe that the simple rescaling method presented in [17] is sufficient and did not require any additional manipulation for the removal of all higher-order poles from the differential equation. The differential equations have been treated with the same recursive expansion method already employed for the generation of the Mellin moments of  $F_2$  and  $F_L$ . The level of expansion achieved for the  $d^{abc}d_{abc}$  color factor gives confidence that this method can be applied also beyond  $n_f^2$ . We leave for an upcoming publication the reconstruction of the analytic expression in  $x$ -space and its study.

#### Acknowledgements

This project is being carried out together with A. Basdew-Sharma, F. Herzog and A. Vogt. This work has been supported by the Vidi grant 680-47-551 of the Dutch Research Council (NWO), the UK Research and Innovation (UKRI) FLF Mr/S03479x/1 and the Consolidated Grant ST/T000988/1 of the UK Science and Technology Facilities Council (STFC).

#### References

- [1] R. L. Workman et al. Review of Particle Physics. *PTEP*, 2022:083C01, 2022. doi: 10.1093/ptep/ptac097.
- [2] A. Accardi et al. Electron Ion Collider: The Next QCD Frontier: Understanding the glue that binds us all. *Eur. Phys. J. A*, 52(9):268, 2016. doi: 10.1140/epja/i2016-16268-9.
- [3] R. Abdul Khalek et al. Science Requirements and Detector Concepts for the Electron-Ion Collider: EIC Yellow Report. *Nucl. Phys. A*, 1026:122447, 2022. doi: 10.1016/j.nuclphysa.2022.122447.
- [4] J. L. Abelleira Fernandez et al. A Large Hadron Electron Collider at CERN: Report on the Physics and Design Concepts for Machine and Detector. *J. Phys. G*, 39:075001, 2012. doi: 10.1088/0954-3899/39/7/075001.

- [5] P. Agostini et al. The Large Hadron–Electron Collider at the HL-LHC. *J. Phys. G*, 48(11): 110501, 2021. doi: 10.1088/1361-6471/abf3ba.
- [6] Paolo Bolzoni, Fabio Maltoni, Sven-Olaf Moch, and Marco Zaro. Higgs production via vector-boson fusion at NNLO in QCD. *Phys. Rev. Lett.*, 105:011801, 2010. doi: 10.1103/PhysRevLett.105.011801.
- [7] Frédéric A. Dreyer and Alexander Karlberg. Vector-Boson Fusion Higgs Production at Three Loops in QCD. *Phys. Rev. Lett.*, 117(7):072001, 2016. doi: 10.1103/PhysRevLett.117.072001.
- [8] J. Currie, T. Gehrmann, E. W. N. Glover, A. Huss, J. Niehues, and A. Vogt. N3LO corrections to jet production in deep inelastic scattering using the Projection-to-Born method. *JHEP*, 05: 209, 2018. doi: 10.1007/JHEP05(2018)209.
- [9] J. Sanchez Guillen, J. Miramontes, M. Miramontes, G. Parente, and O. A. Sampayo. Next-to-leading order analysis of the deep inelastic  $R = \sigma_L / \sigma_{\text{total}}$ . *Nucl. Phys. B*, 353: 337–345, 1991. doi: 10.1016/0550-3213(91)90340-4.
- [10] W. L. van Neerven and E. B. Zijlstra. Order  $\alpha_s^2$  contributions to the deep inelastic Wilson coefficient. *Phys. Lett. B*, 272:127–133, 1991. doi: 10.1016/0370-2693(91)91024-P.
- [11] E. B. Zijlstra and W. L. van Neerven. Order  $\alpha_s^2$  QCD corrections to the deep inelastic proton structure functions  $F_2$  and  $F_L$ . *Nucl. Phys. B*, 383:525–574, 1992. doi: 10.1016/0550-3213(92)90087-R.
- [12] S. Moch and J. A. M. Vermaseren. Deep inelastic structure functions at two loops. *Nucl. Phys. B*, 573:853–907, 2000. doi: 10.1016/S0550-3213(00)00045-6.
- [13] S. Moch, J. A. M. Vermaseren, and A. Vogt. Third-order QCD corrections to the charged-current structure function  $F_3$ . *Nucl. Phys. B*, 813:220–258, 2009. doi: 10.1016/j.nuclphysb.2009.01.001.
- [14] J. Blümlein, P. Marquard, C. Schneider, and K. Schönwald. The massless three-loop Wilson coefficients for the deep-inelastic structure functions  $F_2$ ,  $F_L$ ,  $\chi F_3$  and  $g_1$ . *JHEP*, 11:156, 2022. doi: 10.1007/JHEP11(2022)156.
- [15] B. Ruijl, T. Ueda, J. A. M. Vermaseren, J. Davies, and A. Vogt. First Forcer results on deep-inelastic scattering and related quantities. *PoS*, LL2016:071, 2016. doi: 10.22323/1.260.0071.
- [16] B. Ruijl, T. Ueda, and J. A. M. Vermaseren. Forcer, a FORM program for the parametric reduction of four-loop massless propagator diagrams. *Comput. Phys. Commun.*, 253:107198, 2020. doi: 10.1016/j.cpc.2020.107198.
- [17] A. Basdew-Sharma, A. Pelloni, Franz Herzog, and A. Vogt. Four-loop large- $n_f$  contributions to the non-singlet structure functions  $F_2$  and  $F_L$ . *JHEP*, 03:183, 2023. doi: 10.1007/JHEP03(2023)183.
- [18] J. A. M. Vermaseren. Harmonic sums, Mellin transforms and integrals. *Int. J. Mod. Phys. A*, 14:2037–2076, 1999. doi: 10.1142/S0217751X99001032.

- [19] Johannes Blumlein and Stefan Kurth. Harmonic sums and Mellin transforms up to two loop order. *Phys. Rev. D*, 60:014018, 1999. doi: 10.1103/PhysRevD.60.014018.
- [20] E. Remiddi and J. A. M. Vermaseren. Harmonic polylogarithms. *Int. J. Mod. Phys. A*, 15: 725–754, 2000. doi: 10.1142/S0217751X00000367.
- [21] S. A. Larin, T. van Ritbergen, and J. A. M. Vermaseren. The Next next-to-leading QCD approximation for nonsinglet moments of deep inelastic structure functions. *Nucl. Phys. B*, 427:41–52, 1994. doi: 10.1016/0550-3213(94)90268-2.
- [22] S. A. Larin, Paulo Nogueira, T. van Ritbergen, and J. A. M. Vermaseren. The Three loop QCD calculation of the moments of deep inelastic structure functions. *Nucl. Phys. B*, 492:338–378, 1997. doi: 10.1016/S0550-3213(97)80038-7.
- [23] S. A. Larin and J. A. M. Vermaseren. The  $\alpha_s^3$  corrections to the Bjorken sum rule for polarized electroproduction and to the Gross-Llewellyn Smith sum rule. *Phys. Lett. B*, 259: 345–352, 1991. doi: 10.1016/0370-2693(91)90839-I.
- [24] Long Chen and Michał Czakon. Renormalization of the axial current operator in dimensional regularization at four-loop in QCD. *JHEP*, 01:187, 2022. doi: 10.1007/JHEP01(2022)187.
- [25] W. L. van Neerven and A. Vogt. NNLO evolution of deep inelastic structure functions: The Singlet case. *Nucl. Phys. B*, 588:345–373, 2000. doi: 10.1016/S0550-3213(00)00480-6.
- [26] S. Moch, J. A. M. Vermaseren, and A. Vogt. Nonsinglet structure functions at three loops: Fermionic contributions. *Nucl. Phys. B*, 646:181–200, 2002. doi: 10.1016/S0550-3213(02)00870-2.
- [27] J. Davies, A. Vogt, B. Ruijl, T. Ueda, and J. A. M. Vermaseren. Large- $n_f$  contributions to the four-loop splitting functions in QCD. *Nucl. Phys. B*, 915:335–362, 2017. doi: 10.1016/j.nuclphysb.2016.12.012.
- [28] Paulo Nogueira. Automatic Feynman graph generation. *J. Comput. Phys.*, 105:279–289, 1993. doi: 10.1006/jcph.1993.1074.
- [29] J. A. M. Vermaseren. New features of FORM. 10 2000.
- [30] J. Kuipers, T. Ueda, J. A. M. Vermaseren, and J. Vollinga. FORM version 4.0. *Comput. Phys. Commun.*, 184:1453–1467, 2013. doi: 10.1016/j.cpc.2012.12.028.
- [31] Ben Ruijl, Takahiro Ueda, and Jos Vermaseren. FORM version 4.2. 7 2017.
- [32] J.A.M. Vermaseren. The minus database facility. URL <https://www.nikhef.nl/~form/maindir/others/minus/minus.html>.
- [33] J. A. M. Vermaseren, A. Vogt, and S. Moch. The Third-order QCD corrections to deep-inelastic scattering by photon exchange. *Nucl. Phys. B*, 724:3–182, 2005. doi: 10.1016/j.nuclphysb.2005.06.020.

- [34] S. G. Gorishnii, S. A. Larin, L. R. Surguladze, and F. V. Tkachov. Mincer: Program for Multiloop Calculations in Quantum Field Theory for the Schoonschip System. *Comput. Phys. Commun.*, 55:381–408, 1989. doi: 10.1016/0010-4655(89)90134-3.
- [35] S. A. Larin, F. V. Tkachov, and J. A. M. Vermaseren. The FORM version of MINCER. 9 1991.